

A Homotopy Coordinate Descent Optimization Method for l_0 -Norm Regularized Least Square Problem

Zhenzhen Sun, Yuanlong Yu*
 College of Mathematics and Computer Science
 Fuzhou University
 Fuzhou, Fujian, 350116, China
 yu.yuanlong@fzu.edu.cn

Abstract—This paper proposes a homotopy coordinate descent (HCD) method to solve the l_0 -norm regularized least square (l_0 -LS) problem for compressed sensing, which combine the homotopy technique with a variant of coordinate descent method. Differs from the classical coordinate descent algorithms, HCD provides three strategies to speed up the convergence: warm start initialization, active set updating, and strong rule for active set initialization. The active set is pre-selected using a strong rule, then the coordinates of the active set are updated while those of inactive set are unchanged. The homotopy strategy provides a set of warm start initial solutions for a sequence of decreasing values of the regularization factor, which ensures all iterations along the homotopy solution path are sparse. Computational experiments on simulate signals and natural signals demonstrate effectiveness of the proposed algorithm, in accurately and efficiently reconstructing sparse solutions of the l_0 -LS problem, whether the observation is noisy or not.

Index Terms—Compressed sensing, sparse coding, l_0 -LS, homotopy coordinate descent.

I. INTRODUCTION

Sparse coding (SC) provides a class of algorithms for finding succinct representations of stimuli, which has been developed and applied in many fields over the last two decades, i.e., image denoising [1], [2], feature selection [3], [4], and pattern recognition [5], [6].

In general, sparse coding is based on the idea that, for an observed signal $\mathbf{x} \in R^d$ and an over-complete dictionary $\mathbf{D} \in R^{d \times K}$ ($d \ll K$), \mathbf{x} can be reconstructed by a representation $\boldsymbol{\alpha} \in R^K$ using only a few atoms of the dictionary. More formally, the problem of finding the sparse representation $\boldsymbol{\alpha}$ is formulated as:

$$\min_{\boldsymbol{\alpha}}: \|\mathbf{x} - \mathbf{D}\boldsymbol{\alpha}\|_2^2 + \lambda \|\boldsymbol{\alpha}\|_0, \quad (1)$$

where the l_0 -norm is defined as the number of non-zero elements in a given vector, λ is the regularization factor.

This problem has been proven to be a NP-hard problem, researchers have turned to approximately solve it instead. There are three common methods for approximations/relaxations of

the problem: iterative greedy algorithms [7], l_1 -norm convex relaxation methods (which were called basis pursuit (BP)) [8], and l_p -norm ($0 < p < 1$) relaxation methods [9]–[12]. The most known greedy algorithms are orthogonal matching pursuit (OMP) [13] and its variations, i.e., StOMP [14], MPL [15], [16], RobOMP [17], etc.

BP method replace the l_0 norm with an l_1 norm to make a convex relaxation for the original problem, thus the objective function becomes:

$$\min_{\boldsymbol{\alpha}}: \|\mathbf{x} - \mathbf{D}\boldsymbol{\alpha}\|_2^2 + \lambda \|\boldsymbol{\alpha}\|_1, \quad (2)$$

where the l_1 -norm is defined as the sum of absolute values of all elements in a vector. This method has been proven to give the same solution to (1) when the dictionary satisfies some conditions [18], [19]. Many research works have focused on efficiently solving problem (2), [20] provides a comprehensive review of five representative methods, namely, *Gradient Projection* (GP) [21], [22], *Homotopy* [23], [24], *Iterative Shrinkage-Thresholding* (IST) [25]–[28], *Proximal Gradient* (PG) [29], [30], and *Augmented Lagrange Multiplier* (ALM) [31]. Recently, a kind of pathwise coordinate optimization methods called PICASSO [32]–[34] has been proposed to solve the l_p -LS ($0 < p \leq 1$) problem, which has shown superior empirical performance than other state-of-the-art SC algorithms mentioned above.

Although satisfactory results can be achieved by the approximate/relax methods, from the sparsity perspective, l_0 -norm is more desirable. In recent years, researchers try to solve problem (1) directly, iterative hard thresholding (IHT) [35]–[37] is the most popular method. The IHT methods have strong theoretical guarantees, and the extensive experimental results show that the IHT methods can be used to improve the results generated by other methods. Recently, Dong *et al.* proposed two homotopy iterative hard-thresholding methods (HIHT and AHIHT) in [38], which combine the homotopy technique with IHT. The experimental results show that this two homotopy iterative hard-thresholding methods can improve the solution quality and speed up the convergence effectively.

However, IHT methods update all coordinates of $\boldsymbol{\alpha}$ in parallel thus they need to access all entries of the dictionary

*This work is supported by National Natural Science Foundation of China (NSFC) under grant #61873067.

\mathbf{D} in each iteration for computing a full gradient and a sophisticated line search step. Because of that, they are often not scalable and efficient in practice when K is large. Inspired by PICASSO, this paper proposed a homotopy coordinate descent (HCD) method for solving problem (1) directly, which combines the homotopy technique with a variant of coordinate descent method to calculate and trace the solutions of the regularized problem along a continuous path. What's more, differing from the classical coordinate descent algorithms, HCD just update the coordinates of active set, which can reduce the computational time effectively, especially when the solution is very sparse. Experimental results show that the propose method is more efficient and effective than PICASSO and other homotopy methods.

The rest of this paper is organized as follows. Section II presents the proposed HCD method. In addition, convergence of this method is analyzed. Experimental results are presented in Section III and the conclusions are made in Section IV.

II. THE PROPOSED METHOD

A. Problem Formulation

For the sake of easy statement, problem (1) is rewritten as:

$$\Phi_\lambda(\boldsymbol{\alpha}) = \arg \min_{\boldsymbol{\alpha}} \frac{1}{2} \|\mathbf{x} - \mathbf{D}\boldsymbol{\alpha}\|_2^2 + \lambda \|\boldsymbol{\alpha}\|_0, \quad (3)$$

since the square of l_2 -norm and l_0 -norm are all separable function, this problem can be optimized by classical coordinate descent optimization algorithm. Given $\boldsymbol{\alpha}^t$ at t -th iteration, we select a coordinate i , and then take an exact coordinate minimization step

$$\Phi_\lambda(\alpha_i) = \arg \min_{\alpha_i} \frac{1}{2} \|\mathbf{z}^t - \mathbf{d}_i \alpha_i\|_2^2 + \lambda \|\alpha_i\|_0, \quad (4)$$

where α_i is the i -th element of $\boldsymbol{\alpha}$, \mathbf{d}_i denotes the i -th column of \mathbf{D} , and $\mathbf{z}^t = \mathbf{x} - \mathbf{D}\boldsymbol{\alpha}^t + \mathbf{d}_i \alpha_i^t$ denotes the partial residual.

According to IHT, (4) admits a closed form solution computed by the hard thresholding operator [28], [37]:

$$\alpha_i^{t+1} = \Gamma_{\lambda, i}(\boldsymbol{\alpha}^t) = \begin{cases} s_{L_i}(\alpha_i^t), & \text{if } \|s_{L_i}(\alpha_i^t)\|_2 > \frac{2\lambda}{L_i} \\ 0, & \text{if } \|s_{L_i}(\alpha_i^t)\|_2 \leq \frac{2\lambda}{L_i} \end{cases}, \quad (5)$$

where $s_{L_i}(\alpha_i^t) = \alpha_i^t - \frac{1}{L_i} \nabla f(\alpha_i^t)$, $\nabla f(\alpha_i^t)$ is the gradient of $f(\alpha_i) = \frac{1}{2} \|\mathbf{z}^t - \mathbf{d}_i \alpha_i\|_2^2$ which is Lipschitz continuous (denote its Lipschitz constant as L_{f_i}), constant $L_i > 0$ is an upper bound on the Lipschitz constant, i.e., $L_i \geq L_{f_i}$. We normalize each atom \mathbf{d}_i of \mathbf{D} such that $\|\mathbf{d}_i\|_2 = 1$, thus all L_i can be set as 1 (for convenience, we neglect the index i and use L to replace all L_i in next).

It is time-consumption to update all coordinates, a homotopy coordinate descent optimization framework is proposed to the computational time, which integrates the warm start initialization, active set updating strategy, and strong rule for coordinate pre-selection into the classical coordinate

optimization. These three strategies constitute three nested loops for the proposed algorithm, as illustrated in Fig. 1. For simplicity, we first introduce its inner loop, then its middle loop, and at last its outer loop.

B. Three Loops of HCD

1. *Inner Loop: Iterating over Coordinates within an Active Set.* The inner loop is denoted as active coordinate descent (ActCooDes) algorithm. The iteration index for the inner loop is (t) , where $t = 0, 1, 2, \dots$. The ActCooDes algorithm solves (3) by conducting exact coordinate minimization iteratively, but it only updates a subset of all coordinates, which is called "active set". Accordingly, the complementary set to the active set is called "inactive set", whose coordinates do not change throughout all iterations of the inner loop. Since the active set usually contains few number of coordinates, ActCooDes algorithm is very scalable and efficient.

We denote the active and inactive sets as A and \bar{A} respectively. According to the initial solution of the inner loop $\boldsymbol{\alpha}^{(0)}$, active set and inactive set are selected based on the sparse pattern:

$$A = \{j | \alpha_j^{(0)} \neq 0\} \text{ and } \bar{A} = \{j | \alpha_j^{(0)} = 0\}. \quad (6)$$

Then ActCooDes algorithm minimizes (3) with all coordinates of \bar{A} keeping at zero values, the objective function becomes:

$$\min_{\boldsymbol{\alpha} \in \mathbb{R}^d} \Phi_\lambda(\boldsymbol{\alpha}), \text{ subject to } \boldsymbol{\alpha}_{\bar{A}} = \mathbf{0}. \quad (7)$$

Without loss of generality, we assume $|A| = s$, $A = \{j_1, \dots, j_s\} \subseteq \{1, \dots, K\}$, where $j_1 \leq j_2 \leq \dots \leq j_s$. Given a solution $\boldsymbol{\alpha}^{(t)}$ at t -th iteration, we construct a sequence of auxiliary solutions $\{\mathbf{w}^{(t+1, k)}\}_{k=0}^s$ to obtain $\boldsymbol{\alpha}^{(t+1)}$. Particularly, for $k=0$, we have $\mathbf{w}^{(t+1, 0)} = \boldsymbol{\alpha}^{(t)}$; For $k=1, \dots, s$, we use (5) to update $w_{j_k}^{(t+1, k)}$ and make $w_{\setminus j_k}^{(t+1, k)} = w_{\setminus j_k}^{(t+1, k-1)}$.

Then we set $\boldsymbol{\alpha}^{(t+1)} = \mathbf{w}^{(t+1, s)}$ for the next iteration. The ActCooDes algorithm is terminated when

$$\|\boldsymbol{\alpha}^{(t+1)} - \boldsymbol{\alpha}^{(t)}\|_2 / \|\boldsymbol{\alpha}^{(t)}\|_2 < \tau \lambda, \quad (8)$$

where τ is a small convergence parameter (i.e., 10^{-5}).

The outline of inner loop is presented in Algorithm 1

2. *Middle Loop: Updating Active Sets Iteratively.* Since the inner loop can only converge to a local optimal solution of (7), it is not necessarily the local optimal solution of (3). Therefore, the inner loop needs to be combined with some active set updating scheme, which allows the active set to be changed. This leads to the middle loop of HCD.

The middle loop is denoted as iterative active set updating (IteActUpd) algorithm, and the iteration index for it is $[m]$, where $m = 0, 1, 2, \dots$. As shown in Algorithm 2, the IteActUpd algorithm simultaneously updates the active set and decreases the objective value to ensure that the HCD algorithm converges to a local optimal solution of (3).

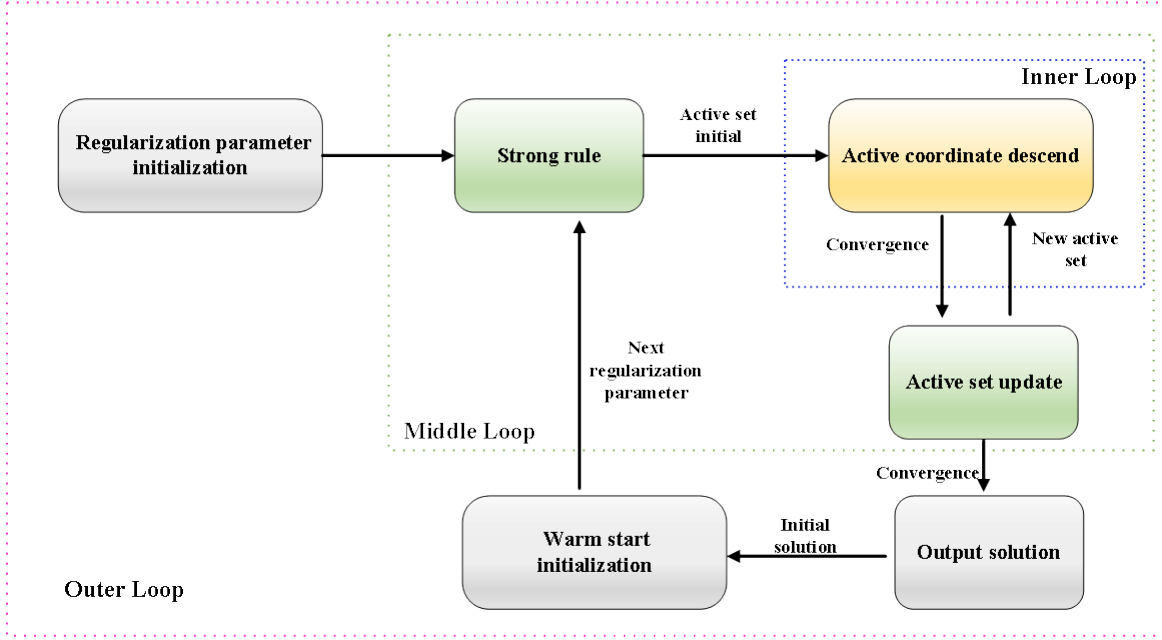


Fig. 1
FRAMEWORK OF HCD.

Algorithm 1 $\hat{\alpha} \leftarrow \text{ActCooDes}(\alpha^{(0)}, \lambda, \tau)$

(Input:) $\alpha^{(0)}, \lambda, \tau$
initialize $t \leftarrow 0, A = \{j | \alpha_j^{(0)} \neq 0\}$;
repeat
 $\mathbf{w}^{(t+1,0)} = \alpha^{(t)}$;
for $k = 1 : s$
 $w_{j_k}^{(t+1,k)} = \Gamma_{\lambda, j_k}(\mathbf{w}^{(t+1, k-1)})$;
 $\mathbf{w}_{j_k}^{(t+1,k)} = \mathbf{w}_{j_k}^{(t+1, k-1)}$
end
 $\alpha^{(t+1)} \leftarrow \mathbf{w}^{(t+1, s)}$;
 $t \leftarrow t + 1$;
until $\|\alpha^{(t+1)} - \alpha^{(t)}\|_2 / \|\alpha^{(t)}\|_2 < \tau \lambda$
 $\hat{\alpha} \leftarrow \alpha^{(t)}$;

(1) Strong Rule for Active Set Initialization: Tibshirani *et al.* [39] suggest a aggressive active set initialization procedure for PICASSO using a "strong rule", which often leads to superior computational performance in practice. Inspired by this, we also propose a "strong rule" for our HCD algorithm to initial active set. Suppose an initial solution $\alpha^{[0]}$ is supplied to the middle loop, given an active set initialization parameter

$\varphi \in (0, 1)$, the strong rule for HCD initializes A_0 and \bar{A}_0 as:

$$A_0 = \left\{ j | \alpha_j^{[0]} = 0, |\nabla_j f(\alpha^{[0]})| \geq (1 - \varphi) \sqrt{\frac{2\lambda}{L}} \right\} \cup \{j | \alpha_j^{[0]} \neq 0\}, \quad (9)$$

$$\bar{A}_0 = \left\{ j | \alpha_j^{[0]} = 0, |\nabla_j f(\alpha^{[0]})| < (1 - \varphi) \sqrt{\frac{2\lambda}{L}} \right\}, \quad (10)$$

where $\nabla_j f(\alpha^{[0]})$ denotes the j -th entry of $\nabla f(\alpha^{[0]})$, and $\nabla f(\alpha)$ is the gradient of $f(\alpha) = \frac{1}{2} \|\mathbf{x} - \mathbf{D}\alpha\|_2^2$. Note that the initialization parameters φ need to be a reasonably small value (i.e., 0.1). Otherwise, the "strong rule" will choose too many active coordinates and affect the sparsity of the solution.

(2) Active Set Updating Strategy: Suppose at the m -th iteration ($m \geq 1$), we obtain a solution $\alpha^{[m]}$ with a pair of active and inactive sets defined as:

$$A_m = \{j | \alpha_j^{[m]} \neq 0\} \text{ and } \bar{A}_m = \{j | \alpha_j^{[m]} = 0\}. \quad (11)$$

Each iteration of IteActUpd algorithm consists of two stages. The first stage is to conduct the ActCooDes algorithm over the active set A_m until convergence, and then return a solution $\alpha^{[m+0.5]}$. Since the coordinate descent algorithm may produce zero values for some active set coordinates, we remove these coordinates from the active set and update the

Algorithm 2 $\hat{\alpha} \leftarrow \text{IteActUpd}(\alpha^{[0]}, \lambda, \delta, \tau, \varphi)$

(Input:) $\alpha^{[0]}, \lambda, \tau, \delta, \varphi$
initialize $A_0 = \left\{ j | \alpha_j^{[0]} = 0, |\nabla_j f(\alpha^{[0]})| \geq (1 - \varphi) \sqrt{\frac{2\lambda}{L}} \right\}$
 $\cup \left\{ j | \alpha_j^{[0]} \neq 0 \right\}, m \leftarrow 0;$
repeat
 $\alpha^{[m+0.5]} \leftarrow \text{ActCooDes}(\alpha^{[m]}, \lambda, \tau);$
 $A_{m+0.5} \leftarrow \left\{ j | \alpha_j^{[m+0.5]} \neq 0 \right\}, \bar{A}_{m+0.5} \leftarrow \left\{ j | \alpha_j^{[m+0.5]} = 0 \right\};$
 $k_m = \arg \max_{k \in \bar{A}_{m+0.5}} |\nabla_k f(\alpha^{[m+0.5]})|;$
 $\alpha_{k_m}^{[m+1]} \leftarrow \Gamma_{\lambda, k_m}(\alpha^{[m+0.5]}), \alpha_{\setminus k_m}^{[m+1]} = \alpha_{\setminus k_m}^{[m+0.5]};$
 $A_{m+1} \leftarrow A_{m+0.5} \cup \{k_m\}, \bar{A}_{m+1} \leftarrow \bar{A}_{m+0.5} \setminus \{k_m\};$
 $m \leftarrow m + 1;$
until $|\nabla_{k_m} f(\alpha^{[m+0.5]})| \leq (1 - \delta) \sqrt{\frac{2\lambda}{L}}$
 $\hat{\alpha} \leftarrow \alpha^{[m]};$

active and inactive sets as follows:

$$\begin{aligned} A_{m+0.5} &= \left\{ j | \alpha_j^{[m+0.5]} \neq 0 \right\}, \\ \bar{A}_{m+0.5} &= \left\{ j | \alpha_j^{[m+0.5]} = 0 \right\}. \end{aligned} \quad (12)$$

The second stage checks which coordinates of $\bar{A}_{m+0.5}$ should be added into the active set. We propose a greedy selection rule for updating the active set. Particularly, let $\nabla_j f(\alpha^{[m+0.5]})$ denote the j -th entry of $\nabla f(\alpha^{[m+0.5]})$, we select a coordinate by

$$k_m = \arg \max_{k \in \bar{A}_{m+0.5}} |\nabla_k f(\alpha^{[m+0.5]})|. \quad (13)$$

The IteActUpd algorithm is terminated if

$$|\nabla_{k_m} f(\alpha^{[m+0.5]})| \leq (1 - \delta) \sqrt{\frac{2\lambda}{L}}, \quad (14)$$

where δ is a small convergence parameter (e.g., 10^{-5}). Otherwise, we take

$$\alpha_{k_m}^{[m+1]} = \Gamma_{\lambda, k_m}(\alpha^{[m+0.5]}) \text{ and } \alpha_{\setminus k_m}^{[m+1]} = \alpha_{\setminus k_m}^{[m+0.5]}, \quad (15)$$

and update the active and inactive set as:

$$A_{m+1} = A_{m+0.5} \cup \{k_m\} \text{ and } \bar{A}_{m+1} = \bar{A}_{m+0.5} \setminus \{k_m\}. \quad (16)$$

The outline of middle loop is presented in Algorithm 2.

3. Outer Loop: Iterating over Regularization Parameter.

The outer loop of HCD is the homotopy strategy which provides a warm starting initialization (WarStaInt). In the outer loop, we first set a large initial value of the regularization parameter λ and gradually decrease it with a common ratio $\eta \in (0, 1)$ until it reach to the target value λ_{tgt} . For every fixed value of the regularization parameter, the IteActUpd algorithm is used to search an approximate optimal solution of (3), which is set as the initial solution of

Algorithm 3 $\hat{\alpha} \leftarrow \text{WarStaInt}(\alpha^0, \lambda_{tgt}, \eta)$

(Input:) $\alpha^0, \lambda_{tgt}, \eta, \tau, \delta, \varphi$
initialize $\lambda_0 = \|\nabla f(\alpha^0)\|_\infty, n \leftarrow 0;$
repeat
 $\lambda_{n+1} = \eta \lambda_n;$
 $\alpha^{n+1} \leftarrow \text{IteActUpd}(\alpha^n, \lambda_{n+1}, \delta, \tau, \varphi);$
 $n \leftarrow n + 1;$
until $\lambda_n \leq \lambda_{tgt}$
 $\hat{\alpha} \leftarrow \alpha^n;$

the next iteration. Usually, the next loop with warm starting will require fewer iterations than current loop [28]. We set the initial regularization parameter as $\lambda_0 = \|\mathbf{D}^T \mathbf{x}\|_\infty$ as with most algorithms. An outline of the WarStaInt algorithm is described as Algorithm 3.

C. Convergence Analysis

For a fixed λ_n , suppose the middle loop iterates to the m -th time and $|A_m| = s$. For $i \in A_m$, it has been proven that [37], [38]

$$\Phi_{\lambda_n}(\alpha_i^{(t+1)}) \leq \Phi_{\lambda_n}(\alpha_i^{(t)}), \quad (17)$$

while for $i \in \bar{A}_m, \Phi_{\lambda_n}(\alpha_i^{(t+1)}) = \Phi_{\lambda_n}(\alpha_i^{(t)})$.

Thus, for all $\alpha_i^{(t+1)}$ ($i = 1, 2, \dots, K$), we have

$$\begin{aligned} \Phi_{\lambda_n}(\alpha^{(t+1)}) &= \sum_{i=1}^K \Phi_{\lambda_n}(\alpha_i^{(t+1)}) \\ &\leq \sum_{i=1}^K \Phi_{\lambda_n}(\alpha_i^{(t)}) = \Phi_{\lambda_n}(\alpha^{(t)}). \end{aligned} \quad (18)$$

It implies that

$$\begin{aligned} \Phi_{\lambda_n}(\alpha^{[m+0.5]}) &= \Phi_{\lambda_n}(\alpha^{[m+0.5, T_{m+0.5}]}) \\ &\leq \Phi_{\lambda_n}(\alpha^{[m+0.5, 0]}) = \Phi_{\lambda_n}(\alpha^{[m]}), \end{aligned} \quad (19)$$

where $T_{m+0.5}$ is the number of iterations of ActCooDes in m -th iteration of middle loop.

Similarly, we have

$$\Phi_{\lambda_n}(\alpha^{[m+1]}) \leq \Phi_{\lambda_n}(\alpha^{[m+0.5]}) \leq \Phi_{\lambda_n}(\alpha^{[m]}), \quad (20)$$

this inequality implies that, for a fixed $\lambda_n, \Phi_{\lambda_n}\{\alpha^{[m]}\}$ is non-increasing. Since $f(\alpha)$ is bounded below, it then follows that $\Phi_{\lambda_n}\{\alpha^{[m]}\}$ is bounded below. Hence, $\Phi_{\lambda_n}\{\alpha^{[m]}\}$ converges to a finite value as $m \rightarrow \infty$ and a local optimal solution $\alpha_{\lambda_n}^*$ can be achieved.

Since the λ is monotone decreased, and $\alpha_{\lambda_n}^*$ is set as the initial solution for IteActUpd in λ_{n+1} , we obtain that:

$$\Phi_{\lambda_n}(\alpha_{\lambda_n}^*) > \Phi_{\lambda_{n+1}}(\alpha_{\lambda_n}^*) = \Phi_{\lambda_{n+1}}(\alpha_{\lambda_{n+1}}^0) \geq \Phi_{\lambda_{n+1}}(\alpha_{\lambda_{n+1}}^*), \quad (21)$$

it implies that the objective value is monotone decreasing and a local optimal solution can be achieved by the proposed algorithm.

III. EXPERIMENT

In this section, we conduct computational experiments for testing the performances of our HCD method on reconstructing sparse representation for observed signal. The proposed method is compared with PICASSO and three state-of-the-art homotopy algorithms, namely PGH [30], HIHT [38] and AHIHT [38]. All experiments are performed on a personal computer with an Intel *Core™* i7-7700 CPU (3.60 GHz) and 32-GB memory, using a MATLAB toolbox.

The experiments are mainly divide into three parts: (1) We evaluate the effectiveness of our algorithm; (2) We evaluate the influence of parameters λ_{gt} and η in the algorithm; (3) We compare the performance of our algorithm with the compared algorithms in generated signals and natural signals.

Suppose $\hat{\alpha}$ is the obtained solution, α^* is the unknown sparse representation, the validation metrics used in our experiments include:

- 1) Reconstruction error: $\varepsilon = \|\mathbf{x} - \mathbf{D}\hat{\alpha}\|_2$;
- 2) Objective gap: $obj_gap = \Phi(\hat{\alpha}) - \Phi^*$, where $\Phi^* = \Phi(\alpha^*)$;
- 3) Sparsity: $nnz = \|\hat{\alpha}\|_0$;
- 4) Reconstruction time: CPU time (in seconds).

A. Data Generation and Parameter Setting

In the experiments, we use normal distribution and uniform distribution to generate simulate signals. For normal distribution, we firstly randomly generated the dictionary $\mathbf{D} \in \mathbb{R}^{d \times K}$ with mean 0 and standard deviation 1, the vector $\alpha^* \in \mathbb{R}^K$ was generated with the same distribution at s randomly chosen coordinates ($\|\alpha^*\|_0 = s$), the noise $\mathbf{z} \in \mathbb{R}^d$ is a dense vector with independent random entries with mean 0 and standard deviation σ . For uniform distribution, the entries of \mathbf{D} are generated independently with the uniform distribution over the interval $[-1, +1]$, the noise is a dense vector with independent random entries with the uniform distribution over the interval $[-\sigma, \sigma]$, where σ is the noise magnitude. Finally, the observed signal $\mathbf{x} \in \mathbb{R}^d$ is generated as $\mathbf{x} = \mathbf{D}\alpha^* + \mathbf{z}$.

For natural signals, we randomly extracted 10 image patches from Barbara and Lena images to generate natural signals. Barbara image is noise-free and Lena image has random gaussian noise with $\sigma = 10$. The patch size of Barbara and Lena are 8×8 and 16×16 , respectively (it means the dimension d of observed signal are 64 and 256, respectively). The dictionary is randomly generated with normal distribution and be normalized, the number of atoms are set as $K = 256$ and $K = 1024$, respectively. The average results of 10 image patches are recorded for comparison.

In the experiments, unless otherwise stated, all parameters are set as follows. The initial value λ_0 of all algorithms is set as $\|\mathbf{D}^T \mathbf{x}\|_\infty$, the initial solution is set as $\alpha^0 = \mathbf{0}$. Other parameters are set as: $\tau = 10^{-6}$, $\delta = 10^{-3}$, $\varphi = 0.05$, $\eta = 0.5$.

B. The Effectiveness of HCD

In this part, we generated normal distributed noise-free signal with ($d = 300, K = 2000, s = 20$) to verify the proposed method, the regularization parameter λ_{gt} is set as 0.01, 20 repeated trials are carried out and average results are recorded. Fig. 2 and Fig. 3 show two cases of the scatter diagram of reconstructed signal and convergence curve, and Tab. I presents the average results on the validation metrics. As it can be seen from Fig. 2(a) and Fig. 3(a) that the solution $\hat{\alpha}$ obtained by our algorithm coincides completely with the original sparse signal α^* , which indicates that our algorithm can achieve the optimal solution and has strong reconstruction performance, the results presented in Tab. I also indicate the effectiveness of our algorithm. From Fig. 2(b) and Fig. 3(b) we can see that, only a dozen iterations can our algorithm convergent to the terminate condition, and from Tab. I we can see the average time spent of our algorithm to reconstruct the sparse signal is only 0.6074 seconds. This two results indicate that the convergence speed of our algorithm is very fast which is applicable in practice.

TABLE I
OTHER PERFORMANCE INDICATORS RESULTS

Metric	Value
ε	$5.1611e-9$
obj_gap	$9.8879e-17$
nnz	20
CPU times	0.6074

C. Parameter Sensitivity

In this part, we investigate the sensitivity of parameters λ_{gt} and η in HCD. First, the normal distributed noisy signal with ($d = 400, K = 2000, s = 30, \sigma = 0.01$) is generated to evaluate the influence of regularization parameter λ_{gt} , the results with different values of λ_{gt} are shown in Fig. 4. From this figure it can be seen that when $\lambda_{gt} = 10^{-3}$ or 10^{-2} , HCD can obtain the same solution. While when $\lambda_{gt} = 10^{-1}$, the solution obtained is a litter more sparse than original sparse signal and results in a large objective gap, but is still acceptable. Therefore, within a certain range of λ_{gt} , it only has a great influence on the number of iterations which will not influence the final result. In particular, it can be seen from Fig.4(b) that, despite λ_{gt} is changed, HCD traced the same solution path in previous iterations. The experimental results show that the proposed algorithm is robust to the regularization parameter, and it is unnecessary to spend too much time on parameter tuning.

In order to evaluate the influence of η in HCD, we generated uniform distributed noisy signal with ($d = 500, K = 2000, s = 50, \sigma = 0.01$) to do the experiment, the results with different values of η are shown in Fig. 5. It can be seen from this figure that, though different values of η can get similar results, the number of iterations of the algorithm gradually

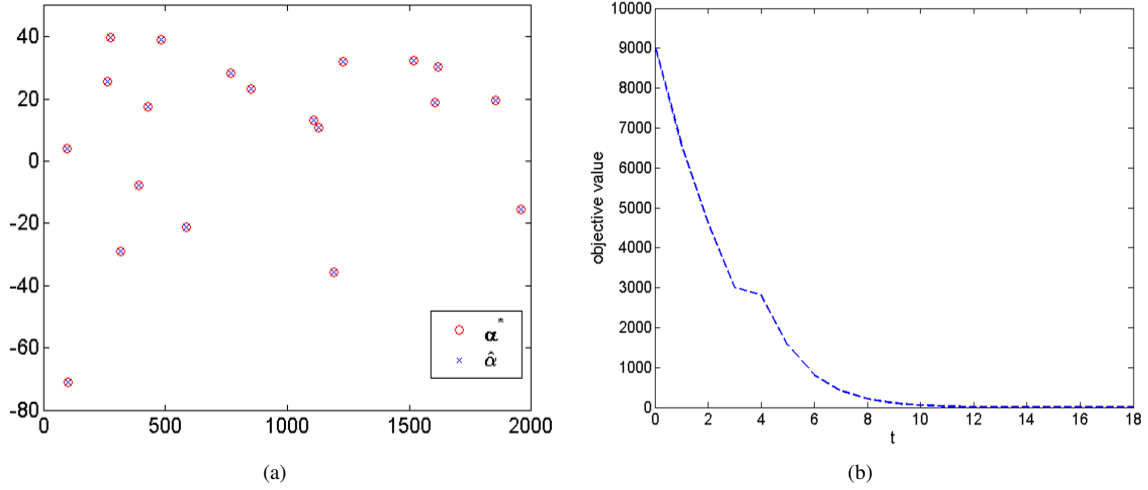


Fig. 2

RECONSTRUCTION RESULTS (CASE ONE). (A) SCATTER DIAGRAM OF ORIGINAL SPARSE SIGNAL AND RECONSTRUCTED SIGNAL. (B) CONVERGENCE CURVE.

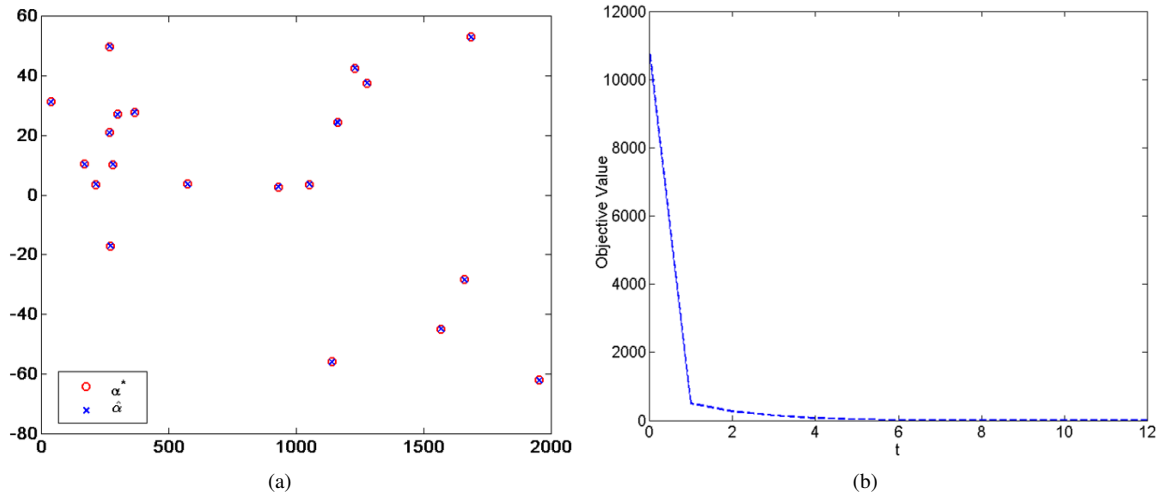


Fig. 3

RECONSTRUCTION RESULTS (CASE TWO). (A) SCATTER DIAGRAM OF ORIGINAL SPARSE SIGNAL AND RECONSTRUCTED SIGNAL. (B) CONVERGENCE CURVE.

increases as η increases. However, if η is too small (i.e., 0.2), the gap between two adjacent values of λ is too large, which will make HCD take more time to search for the solution (the CPU time of HCD with respect to these three values of η are 2.44s, 1.47s and 1.79s, respectively). Therefore, for the following experiments, η is set as 0.5.

D. Comparison Results

In this part, we show the superiority of our algorithm comparing with state-of-the-art SC algorithms. (1) Generated

signal: we generated normal distributed noisy signal with $(d = 256, K = 1024, s = 32, \sigma = 0.01)$ and uniform distributed noisy signal with $(d = 1000, K = 5000, s = 100, \sigma = 0.01)$ for comparison. In the first case, the λ_{gt} of HCD, HIHT and AHIHT are set as 0.01 while it is set as 0.1 for PICASSO and PGH in order to get sparse solution. In the second case, λ_{gt} is set as 0.01 for HCD, HIHT and AHIHT, and 0.5 for PICASSO and PGH. The performance results of each algorithm are shown in Fig. 6 and Fig. 7, respectively.

Fig. 6(a) shows the objective gap versus the number of

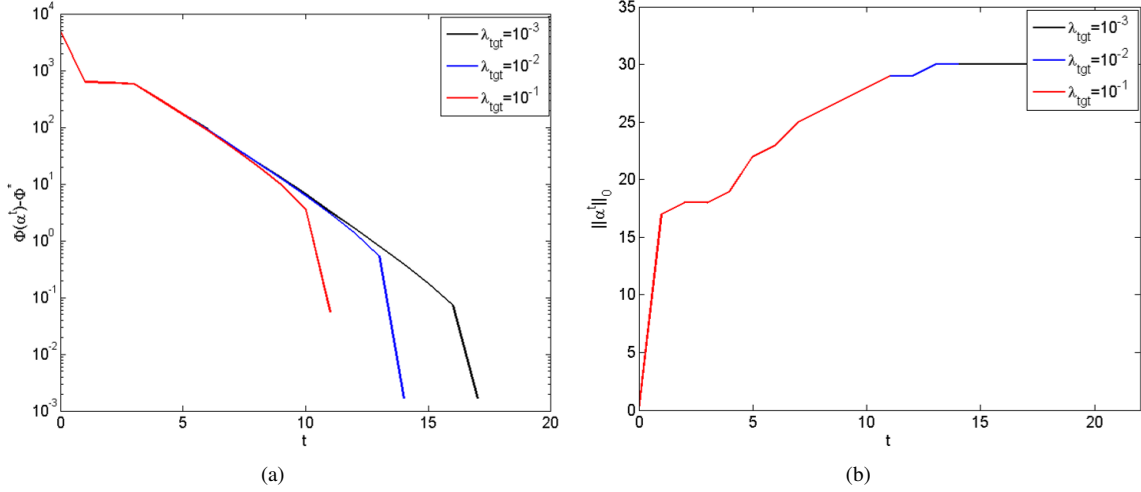


Fig. 4

PERFORMANCE OF THE HCD METHOD BY VARYING λ_{tgt} . (A): *obj_gap*. (B): SPARSITY ALONG SOLUTION PATH.

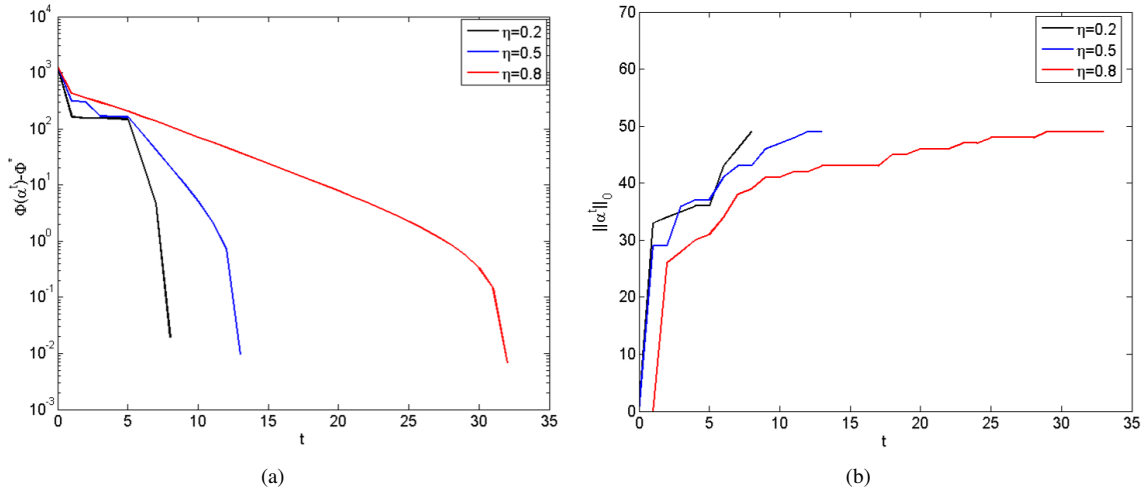


Fig. 5

PERFORMANCE OF THE HCD METHOD BY VARYING η . (A): *obj_gap*. (B): SPARSITY ALONG SOLUTION PATH.

iterations t , from it we can see that HCD can obtain the lowest *obj_gap* than the other four algorithms. From Fig. 6(b) it can be seen that PGH obtained a much larger reconstruction error than the other four algorithms, while the other four algorithms get similar results. It can be seen from Fig. 6(c) that, the sparsity of the sequences $\{\alpha^t\}$ generated by PGH and HIHT algorithms oscillate much during the iteration process. However, the sparsity generated by HCD, AHIHT and PICASSO do not oscillate, and is almost increasing with the number of iterations, they are always searching the solution in a sparse path. Fig. 6(d) shows the number of iterations of each λ_n . We can see that all stages of HCD and AHIHT

took only 1 inner iterations and PICASSO took only 1 to 3 inner iterations to reach the relative precision, while PGH and HIHT took much inner iterations at each stage. We can make the conclusion that the two kinds of coordinate descent methods and AHIHT are more effective and efficient in reconstructing sparse representation than PGH and HIHT, while HCD and AHIHT are even better than PICASSO, this proves that l_0 -norm is more effective than l_p -norm ($0 < p \leq 1$) in reconstructing sparse representation. Fig. 7 demonstrates the same conclusion as Fig. 6

(2) Natural signal: In this experiment, λ_{tgt} is set as 0.01 for HCD and HIHT, while for PGH and PICASSO it is set

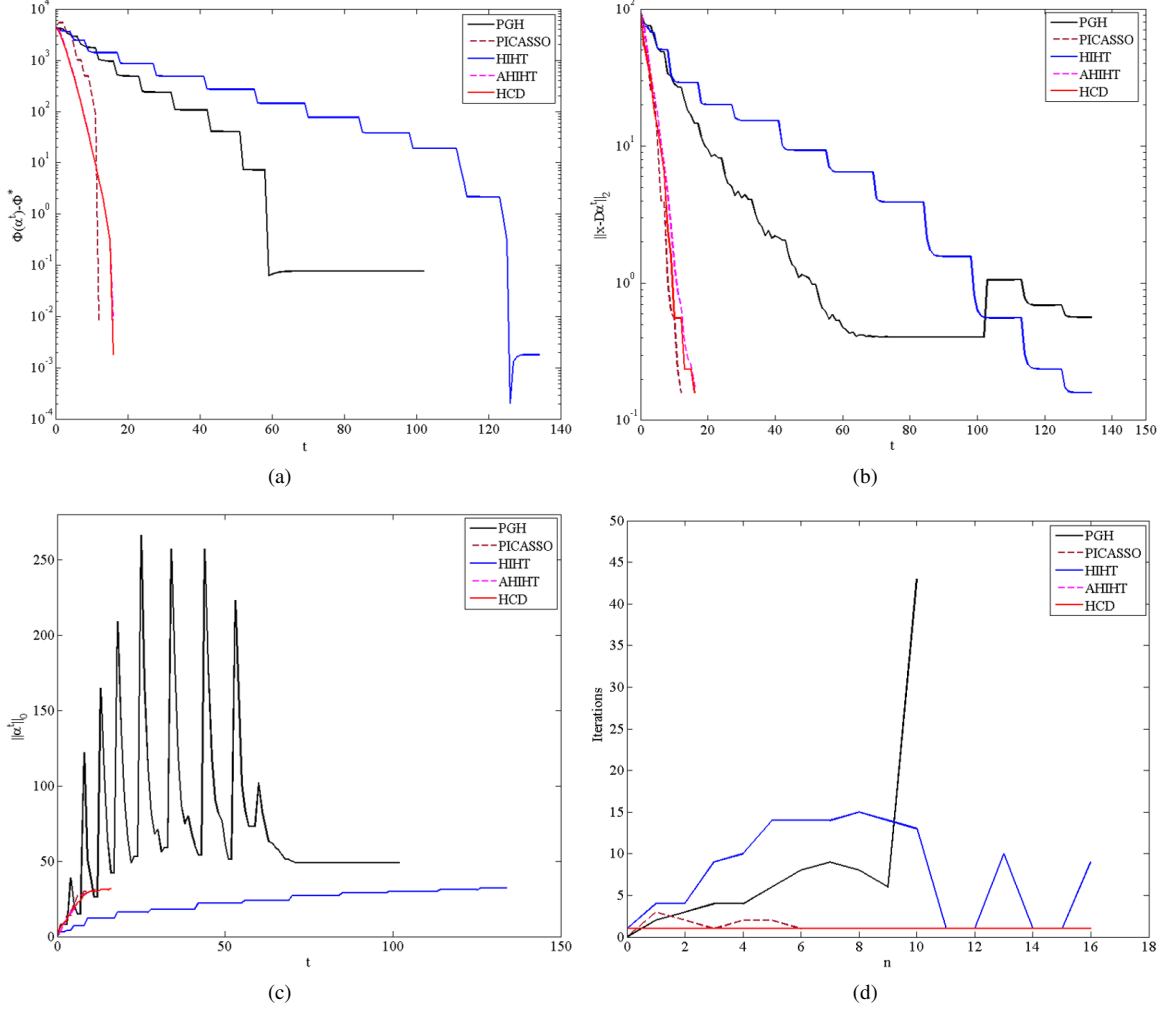


Fig. 6

PERFORMANCE OF THE COMPARED METHODS ON NORMAL DISTRIBUTED NOISY SIGNAL. (A): *obj_gap*. (B): RECONSTRUCTION ERROR. (C): SPARSITY ALONG SOLUTION PATH. (D): NUMBER OF ITERATIONS OF EACH λ_n .

as 0.1, and it is tuned for AHIHT to get a reasonable result. Since α^* is unknown, we compare these algorithms in terms of reconstruction error, sparsity and reconstruction time, the results are shown in Tab. II. It can be seen from this table that, AHIHT fails to produce sparse representation for nature signal when the atoms of dictionary are normalized ($\|d_i\|_2 = 1, \forall i$), while this condition is always made in practical applications to avoid trivial solution. Compared with PGH, the other three algorithms can get a more sparse solution while maintain a lower reconstruction error, indicating that the other three algorithms can obtain a better local optimal solution. Compared with HIHT, PICASSO and HCD have improved the performance of sparse coding when applied in image reconstruction, while HCD is ever better than PICASSO. In term of reconstruction time, HIHT gets the lowest

computational time (except AHIHT) due to HIHT updates all coordinates in parallel, while the computational time of our algorithm is also acceptable. For high-dimensional data, HCD has achieved a significant reduction in computational time compared with PICASSO, indicating that HCD is more suitable than PICASSO for learning the sparse representation for high-dimensional signals and more applicable in practice. Therefore, compared with the other four algorithms, our algorithm achieves a better balance between reconstruction performance and computational time, and can learn the sparse representation for natural signal more effectively.

IV. CONCLUSIONS

This paper proposed a homotopy coordinate descent algorithm to solve the l_0 -norm regularized least square problem in

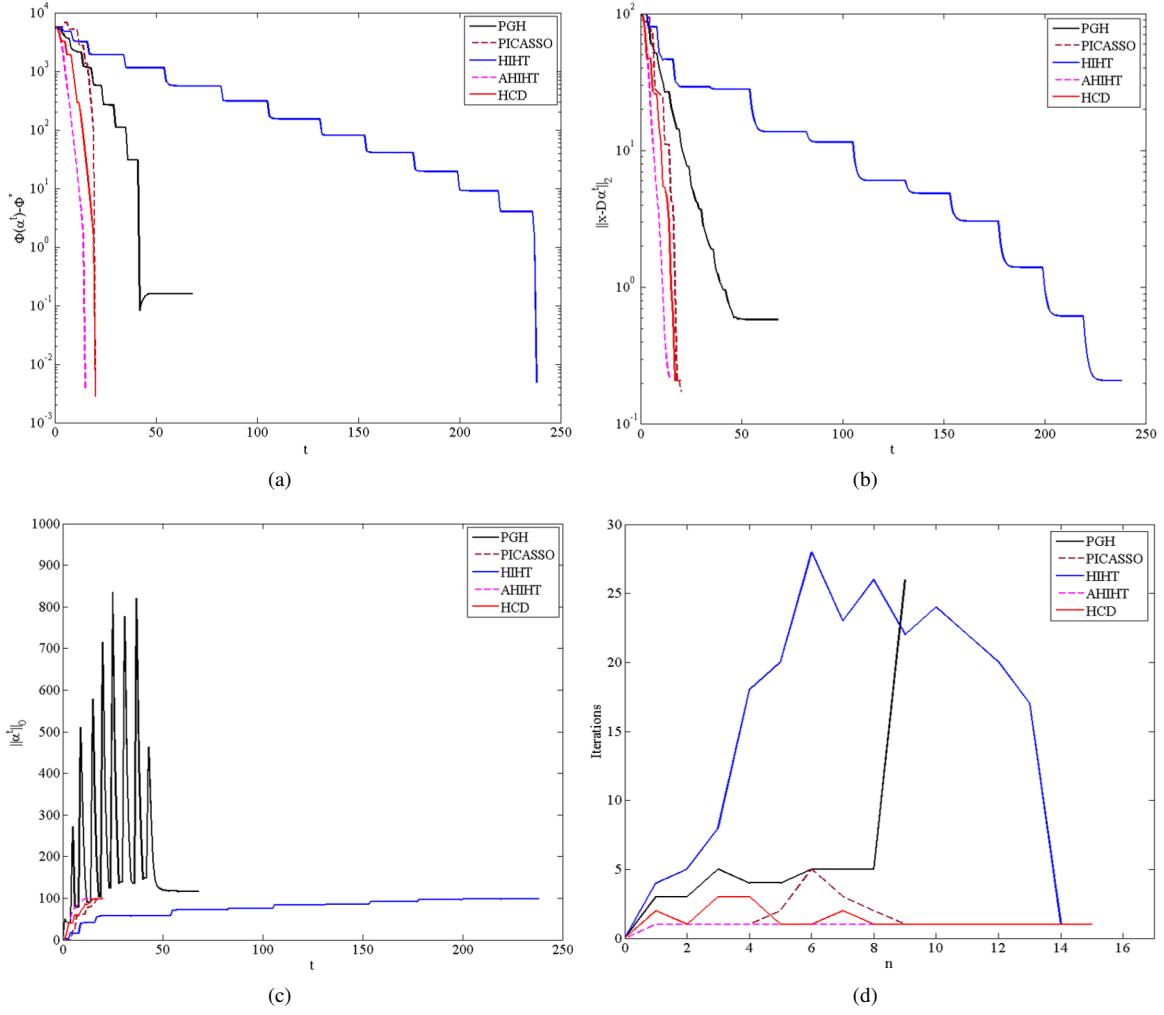


Fig. 7

PERFORMANCE OF THE COMPARED METHODS ON UNIFORM DISTRIBUTED NOISY SIGNAL. (A): obj_gap . (B): RECONSTRUCTION ERROR. (C): SPARSITY ALONG SOLUTION PATH. (D): NUMBER OF ITERATIONS OF EACH λ_n .

TABLE II
AVERAGE RESULTS OF EACH ALGORITHM IN NATURAL SIGNALS

Algorithm	Barbara ($d = 64, K = 256$)			Lena ($d = 256, K = 1024$)		
	ε	nnz	Times	ε	nnz	Times
PGH	0.0925	51.75	0.6463	0.0667	209.14	1.2278
PICASSO	0.0238	44.0	0.0962	0.0329	146.36	2.5695
HIHT	0.0428	46.6	0.0993	0.0388	161.93	0.3326
AHIHT	0.8177	74.43	0.0009	0.1360	248.57	0.0048
HCD	0.0182	47.1	0.1074	0.0343	143.21	0.7613

sparse coding. Differs from the classical coordinate descent algorithms, the proposed algorithm provides three strategies to speed up the convergence: warm start initialization, active set updating, and strong rule for active set initialization. Extensive computational experiments in generated signals and natural signals demonstrate that the proposed algorithm can efficiently and effectively solve the l_0 -LS problem no matter whether the observation is noisy or not. Moreover, our algorithm perform better than four state-of-the-art homotopy methods PGH, HIHT, AHIHT and PICASSO, in both computational time and solution quality.

REFERENCES

- [1] C. L. P. Chen, L. Liu, L. Chen, Y. Y. Tang, and Y. Zhou, "Weighted couple sparse representation with classified regularization for impulse noise removal," *IEEE Transactions on Image Processing*, vol. 24, no. 11, pp. 4014–4026, 2015.
- [2] L. Liu, C. L. P. Chen, X. You, Y. Y. Tang, Y. Zhang, and S. Li, "Mixed noise removal via robust constrained sparse representation," *IEEE Transactions on Circuits and Systems for Video Technology*, vol. 28, no. 9, pp. 2177–2189, 2018.
- [3] R. Tibshirani, "Regression shrinkage and selection via the lasso," *Journal of the Royal Statistical Society: Series B (Methodological)*, vol. 58, no. 1, 1996.
- [4] T. Pang, F. Nie, J. Han, and X. Li, "Efficient feature selection via $l_{2,0}$ -norm constrained sparse regression," *IEEE Transactions on Knowledge and Data Engineering*, vol. 31, no. 5, pp. 880–893, 2019.
- [5] Z. Jiang, Z. Lin, and L. S. Davis, "Label consistent k-svd: Learning a discriminative dictionary for recognition," *IEEE Transactions on Pattern Analysis and Machine Intelligence*, vol. 35, no. 11, pp. 2651–2664, 2013.
- [6] N. Akhtar and A. Mian, "Nonparametric coupled bayesian dictionary and classifier learning for hyperspectral classification," *IEEE Transactions on Neural Networks and Learning Systems*, vol. 29, no. 9, pp. 4038–4050, 2018.
- [7] S. Mallat and Z. Zhang, "Matching pursuits with time-frequency dictionaries," *IEEE Transactions on Signal Processing*, vol. 41, no. 12, pp. 3397–3415, 1993.
- [8] S. Chen, D. Donoho, and M. Saunders, "Atomic decomposition by basis pursuit," *SIAM Review*, vol. 43, no. 1, pp. 129–159, 2001.
- [9] R. Chartrand, "Exact reconstruction of sparse signals via nonconvex minimization," *IEEE Signal Processing Letters*, vol. 14, no. 10, pp. 707–710, 2007.
- [10] Z. Xu, X. Chang, F. Xu, and H. Zhang, " $l_{1/2}$ regularization: A thresholding representation theory and a fast solver," *IEEE Transactions on Neural Networks and Learning Systems*, vol. 23, no. 7, pp. 1013–1027, 2012.
- [11] X. Chen, M. K. Ng, and C. Zhang, "Non-lipschitz l_p -regularization and box constrained model for image restoration," *IEEE Transactions on Image Processing*, vol. 21, no. 12, pp. 4709–4721, 2012.
- [12] L. Qin, Z. C. Lin, Y. She, and Z. Chao, "A comparison of typical l_p minimization algorithms," *Neurocomputing*, vol. 119, no. 16, pp. 413–424, 2013.
- [13] Y. C. Pati, R. Rezaifar, and P. Krishnaprasad, "Orthogonal matching pursuit: recursive function approximation with applications to wavelet decomposition." in *IEEE International Conference on Signal, Systems and Computers*, vol. 1, 1993, pp. 40–44.
- [14] D. L. Donoho, Y. Tsaig, I. Drori, and J. L. Starck, "Sparse solution of underdetermined systems of linear equations by stagewise orthogonal matching pursuit," *IEEE Transaction on Information Theory*, vol. 58, no. 2, pp. 1094–1121, 2012.
- [15] M. K. Tan, I. W. Tsang, and L. Wang, "Matching pursuit lasso part i: Sparse recovery over big dictionary," *IEEE Transaction on Signal Processing*, vol. 68, no. 3, pp. 723–741, 2015.
- [16] —, "Matching pursuit lasso part ii: Applications and sparse recovery over batch signals," *IEEE Transaction on Signal Processing*, vol. 68, no. 3, pp. 742–753, 2015.
- [17] C. A. Loza, "Robomp: Robust variants of orthogonal matching pursuit for sparse representations," *PeerJ Computer Science*, vol. 5, p. e192, 2019.
- [18] D. Donoho and M. Elad, "Optimally sparse representation in general (nonorthogonal) dictionaries via l^1 minimization." in *Proceeding of the National Academy of Sciences of the United States of America*, vol. 100, no. 5, 2003, pp. 2197–2202.
- [19] E. J. Candes and T. Tao, "Near-optimal signal recovery from random projections: Universal encoding strategies?" *IEEE Transactions on Information Theory*, vol. 52, no. 12, pp. 5406–5425, 2006.
- [20] A. Y. Yang, A. Ganesh, Z. H. Zhou, S. S. Sastry, and Y. Ma, "A review of fast l_1 -minimization algorithm for robust face recognition," *Proceedings of the International Conference on Computer Vision and Pattern Recognition*, pp. 1–36, 2010.
- [21] M. A. T. Figueiredo, R. D. Nowak, and S. J. Wright, "Gradient projection for sparse reconstruction: Application to compressed sensing and other inverse problems," *IEEE Journal of Selected Topics in Signal Processing*, vol. 1, no. 4, pp. 586–597, 2007.
- [22] S. J. Kim, K. Koh, and S. Boyd, "An interior-point method for large-scale l_1 -regularized least squares," *IEEE Journal on Selected Topics in Signal Processing*, vol. 1, no. 4, pp. 606–617, 2007.
- [23] M. C. D. Malioutov and A. Willsky, "Homotopy continuation for sparse signal representation," *Proceedings of the IEEE International Conference on Acoustics, Speech, and Signal Processing*, 2005.
- [24] B. P. M. Osborne and B. Turlach, "A new approach to variable selection in least squares problems," *IMA Journal of Numerical Analysis*, vol. 20, pp. 389–404, 2000.
- [25] P. Combettes and V. Wajs, "Signal recovery by proximal forward-backward splitting," *SIAM Multiscale Modeling and Simulation*, vol. 4, pp. 1168–1200, 2005.
- [26] M. D. I. Daubechies and C. Mol, "An iterative thresholding algorithm for linear inverse problems with a sparsity constraint," *Communications on Pure and Applied Math*, vol. 57, pp. 1413–1457, 2004.
- [27] E. T. Hale, W. Yin, and Y. Zhang, "A fixed-point continuation method for l_1 -regularized minimization with applications to compressed sensing," *CAAM Tech Report TR07-07*, pp. 1–45, 2007.
- [28] R. N. S. J. Wright and M. Figueiredo, "Sparse reconstruction by separable approximation," *IEEE Transactions on Signal Processing*, vol. 57, no. 7, pp. 2479–2493, 2009.
- [29] A. Beck and M. Teboulle, "A fast iterative shrinkage-thresholding algorithm for linear inverse problems," *SIAM Journal on Imaging Sciences*, vol. 2, no. 1, pp. 183–202, 2009.
- [30] X. Lin and Z. Tong, "A proximal-gradient homotopy method for the sparse least-squares problem," *SIAM Journal on Optimization*, vol. 23, no. 2, pp. 1062–1091, 2013.
- [31] J. Yang and Y. Zhang, "Alternating direction algorithms for l_1 -problems incompressive sensing," (preprint) *arXiv:0912.1185*, 2009.
- [32] X. G. Li, J. Ge, H. M. Jiang, M. D. Wang, M. Y. Hong, and T. Zhao, "Boosting pathwise coordinate optimization in high dimensions: Sequential screening and proximal sub-sampled newton algorithm," *Technical report, Georgia Tech*, 2017.
- [33] T. Zhao, H. Liu, and T. Zhang, "Pathwise coordinate optimization for nonconvex sparse learning: Algorithm and theory," *Annals of Statistics*, 2017.
- [34] J. Ge, X. G. Li, H. M. Jiang, H. Liu, T. Zhang, M. Y. Hong, and T. Zhao, "Picasso: A sparse learning library for high dimensional data analysis in r and python," *Journal of Machine Learning Research*, vol. 20, pp. 1–5, 2019.
- [35] T. Blumensath and M. E. Davie, "Iterative thresholding for sparse approximations," *Fourier Analysis and Applications*, vol. 27, no. 5, pp. 629–654, 2008.
- [36] —, "Iterative hard thresholding for compressed sensing," *Applied and Computational Harmonic Analysis*, vol. 27, no. 3, pp. 265–274, 2009.
- [37] Z. S. Lu, "Iterative hard thresholding methods for l_0 regularized convex cone programming," *Mathematical Programming*, vol. 147, pp. 125–154, 2012.
- [38] Z. Dong and W. Zhu, "Homotopy methods based on l_0 -norm for compressed sensing," *IEEE Transactions on Neural Networks and Learning Systems*, vol. 29, no. 4, pp. 1132–1146, 2018.

- [39] R. Tibshirani, J. Bien, J. Friedman, T. Hastie, N. Simon, J. Taylor, and R. J. Tibshirani, "Strong rules for discarding predictors in lasso-type problems," *Journal of the Royal Statistical Society. Series B, Statistical methodology*, vol. 74, no. 2, pp. 245–266, 2012.